Computers and Concrete, *Vol. 24, No. 5* (*2019*) *413-422*
DOI: https://doi.org/10.12989/cac.2019.24.5.413

Development of 3D Meso-Scale finite element model to study the mechanical behavior of steel microfiber-reinforced polymer concrete

J. Esmaeili* and K. Andalibi[a]

Department of Civil Engineering, University of Tabriz, 29 Bahman Blvd., Tabriz, Iran

(*Received January 20, 2019, Revised September 25, 2019, Accepted October 5, 2019*)

Abstract. In this study, 3D Meso-scale finite-element model is presented to study the mechanical behavior of steel microfiber-reinforced polymer concrete considering the random distribution of fibers in the matrix. The composite comprises two separate parts which are the polymer composite and steel microfibers. The polymer composite is assumed to be homogeneous, which its mechanical properties are measured by performing experimental tests. The steel microfiber-polymer bonding is simulated with the Cohesive Zone Model (CZM) to offer more-realistic assumptions. The CZM parameters are obtained by calibrating the numerical model using the results of the experimental pullout tests on an individual microfiber. The accuracy of the results is validated by comparing the obtained results with the corresponding values attained from testing the steel microfiber-reinforced polymer concrete incorporating 0, 1 and 2% by volume of microfibers, which indicates the excellent accuracy of the current proposed model. The results show that the microfiber aspect ratio has a considerable effect on the mechanical properties of the reinforced polymer concrete. Applying microfibers with a higher aspect ratio improves the mechanical properties of the composite considerably especially when the first crack appears in the polymer concrete specimens.

Keywords: Meso-scale finite-element model; polymer concrete; steel-microfiber; mechanical properties

1. Introduction

As the most common construction material, concrete is steadily affected by environmental damages and various loadings. Given the poor performance of concrete under tensile loadings, different methods, such as using adhesives, additives, aggregates, reinforcement, and new materials, have been tried to improve its properties. Polymer concrete composites have gained much scientific attention in recent years due to their outstanding tensile and compressive strength, flexibility, and high-energy absorption. This includes extensive experimental and numerical studies addressing the mechanical behavior of polymer concrete composites. Polymer concrete is not like traditional concrete, although it uses some of the same types of materials. It is also used for construction projects in the same manner, but the polymer compounds give the concrete several characteristics that tend to make it safer or more durable than regular concrete. Polymer concrete is measured more specifically in terms of density and shrinkage.

Extensive theoretical and experimental studies have focused on determining the mechanical properties of polymer concrete. (Shokrieh *et al*. 2017, Moodi *et al*. 2018, Jafari *et al*. 2018, Martinez *et al*. 2011, Vogt *et al*. 2018) As an example, Jafari *et al*. (2018) examined the effects of the polymer content on the mechanical properties of polymer concrete by conducting experimental tests. They tested specimens with three different epoxy resin contents (10, 12, and 14 wt.%) at various temperatures, and found out that compressive strength of the specimens increases considerably with increasing the resin ratio and aggregates size.

Rebeiz *et al*. (2004) studied the effect of fly ash additives on compressive strength of the polymer concrete and showed that incorporating 15 wt.% fly ash increases compressive strength of the concrete by 95 MPa. Sett and Vipulanandan (2004) studied the properties of polyester-resin-based polymer concrete and glass-fiber-reinforced polymer concrete, addressing the impact of several parameters, including the effect of stress, strain, the elastic modulus, Poisson's ratio, the maximum stress, and the maximum strain on mechanical properties of the concrete. Hassani *et al*. (2018) studied Mechanical properties of epoxy/basalt polymer concrete by using experimental and analytical study. Abdel-Fattah and El-Hawary (1999) studied the flexural strength of the polymer concrete using different resin contents and various types of resins. Martinez *et al*. (2013) investigate Effect of the marble particle sizes, and high gamma radiation doses of Polyester polymer concrete Gencel *et al*. (2012) studied Mechanical properties of polymer concretes containing different amount of hematite or colemanite. Reis and Ferreira (2004) used carbon and glass fibers to improve the fracture and flexural properties of polymer concrete. The study shows that incorporating a small amount of fiber (up to 2%) improves the ductility of polymer concrete by nearly 13%. In another study Reis (2006), they addressed the enhancement of flexural properties of the polymer concrete using natural

*Corresponding author, Associate Professor
E-mail: J-esmaeili@tabrizu.ac.ir
[a]Ph.D. Student
E-mail: k.andalibi@tabrizu.ac.ir

http://www.techno-press.org/?journal=cac&subpage=8

ISSN: 1598-8198 (Print), 1598-818X (Online)

fibers. The study compares the fiber-reinforced and non-reinforced polymer concrete. Their results suggest that natural fibers are effective in improving flexural strength of concrete.

Mechanical properties of the polymer concrete highly depend on the microstructural attributes, such as the sizes, shape, volume ratio, and distribution of the aggregates, Therefore an experimental attempt to determine mechanical properties is time-consuming and costly. As a result, numerical approaches to characterize composite materials have become quite popular. Meso-scale modeling is state of the art, finite-element method that helps to examine the behavior of composite materials conveniently. This method poses no limitation on the type of material and the number or the geometry of its constituents. Hence, the Meso-scale finite-element model is a suitable tool for determining the mechanical properties and the behavior of composite materials under various loading conditions (Tregger *et al*. 2007, Du *et al*. 2012, Wang and Bao 2015, Tam and Lau 2016). Meso-scale modeling is useful in structural characterization of matrix-fiber interactions in steel-fiber-reinforced polymer concrete. Many researchers have studied the behavior of fiber-concrete paste interface. In an experimental study, Shannag *et al*. (1997) examined the steel fiber pullout from a cement-based composite. Isla *et al*. (2015) experimentally studied the steel fiber pullout with different geometries in different composites tests. The study shows that the fiber geometry has a considerable impact on the pullout force, and consequently, fiber-concrete adhesion. In separate studies (Tuyan 2012, Soetens *et al*. 2013, Smolčić and Ožbolt 2017) examined the steel fiber pullout, claiming that the hooked-end fibers outperform flat-end ones. In a numerical study. Aslani and Nejadi (2012) addressed the adhesion of the steel fibers to Self-Compacting Concrete (SCC). They showed that the adhesion between the fibers and the concrete matrix depends on several factors, including the fiber direction, fiber embedding length, fiber geometry, and matrix strength. Therefore, to allow the modeled concrete and fibers to function accurately, the numerical method must portray the characteristics of this region correctly. Karimzadeh *et al*. (2007) proposed a computational modeling procedure to estimate the mechanical behavior of polymer/nanotube composite that models the nanotube-matrix interaction using the continuum mechanics theory and the finite-element method. Ayatollahi *et al*. (2011) proposed to estimate the nonlinear properties of polymer nanocomposite under tensile, flexural, and torsional loading conditions by multi-scale modeling. In their model, the intermediate phase was modeled continuously, and with different Young's modulus assumed for it. The results show the mechanical properties of the fiber-matrix interface to have a negligible impact on the stiffness of the nanocomposite, but fiber aspect ratio to have a significant effect on its Young's modulus.

Several numerical studies have been carried out aiming the understanding of micromechanical behavior of the fiber-matrix system using different techniques, such as the boundary elements method (Budhe *et al*. 2017, París *et al*. 2017, Velasco *et al*. 2018), the developed finite-element method, smeared crack method, and fracture mechanics, to analyze separation at the contact area and, subsequently, the propagation of the fracture into the matrix. One of the most recent studies in the field belongs to Khani *et al*. (2016) who examined elastic properties of the composites reinforced by spiral and string carbon fibers using the multi-scale finite-element method and by considering the different constituents. They introduced a new algorithm to model the random distribution of particles in a polymer matrix and derived results using ABAQUS commercial code considering the particle-matrix interactions. Some studies have used finite-element cohesive zone models to simulate the fiber-matrix interface and study the formation and growth of separation at the zone. A review of the literature on the application of the Cohesive Zone Model (CZM) to model the interface in composite materials reveals the excellent accuracy of the model in estimating the fiber-matrix adhesion. For example, Bouhala *et al*. (2015) established failure parameters of composites using an inverse method based on the CZM, and the finite-element method. This method assumes a zero thickness for the interface elements and simulates the fiber-matrix separation behavior by establishing the fracture properties. Given the accuracy of this method, the CZM was also used in the present study to model the fiber-matrix interface.

In the present study, first, a new mix was proposed to improve the mechanical properties of polymer concrete. The mixture incorporates epoxy resin for the adherence of the polymer concrete constituents. The tensile strength, density, and Young's modulus of the composite were also measured experimentally. Then, considering the mechanical properties obtained, a Meso-scale finite-element method was proposed to model the steel-microfiber-reinforced polymer concrete using ABAQUS-commercial code. This study, for the first time, establishes the mechanical properties of microfiber-reinforced polymer concrete using the Meso-scale model. The CZM was also employed to simulate microfiber- composite interactions, and the model constants were determined using the results from the fiber pullout test. Then, the impact of different parameters, such as fibers content (vol %), aspect ratio, and distribution, on mechanical properties of the polymer concrete was examined by simulating the polymer concrete and the fibers separately, using the Meso-scale model. Finally, the numerical and experimental results were compared, and the accuracy of the model is discussed to evaluate the results of the presented micromechanical model.

2. Experimental program

The polymer concrete used in this study prepared from the combination of Epoxy resin, fillers, steel microfiber, and silica sand. DIGLYCIDYL ETHER OF BISPHENOL A, as epoxy resin and MODIFIED ALIPHATIC AMINE, as the hardening agent are mixed with ratio of 1:2 by weight. The specific gravities of resin and hardener are 1.15 g/cm^3 and 1.03 g/cm^3, respectively.

The aggregates used in the polymer concrete were mainly silica sand due to their compatibility with the epoxy resin and the excellent adhesion between the aggregates and the epoxy resins used in the polymer concrete. Smooth copper-coated steel microfibers with a diameter of 0.2 mm,

Table 1 The Mechanical properties of polymer concrete

Test Item	Unit	Result
Tensile Strength	MPa	10.2
Flexural Strength	MPa	15.7
Compressive Strength	MPa	126
Compressive Modulus of Elasticity	GPa	62

Table 2 The mix proportion of polymer concrete matrix

Specimen No	Cement (kg/m^3)	Micro silica (kg/m^3)	Resin epoxy (kg/m^3)	Sand (kg/m^3)	Fibers (by volume)
PC0	500	100	350	1098	0%
PC1	500	100	350	1098	1%
PC2	500	100	350	1098	2%

length of 12 mm, and elastic modulus of 198 GPa were used in the mixes. Cement and micro silica were used as fillers in polymer concrete compounds. The polymer consisted of two phases, resin, and hardener, and is mixed for about three minutes. The polymer is then mixed with aggregates, cement, and micro silica for another 5 minutes. This procedure continues until all the aggregates and fillers are coated with polymer, then the mixture is poured into the molds. The specimens are kept in molds for 24 hours at room temperature (approximately 25°C) and then stored at 35°C for five days. The laboratory specimens were prepared and tested at three different fibers contents of 0, 1, and 2 vol%. Table 1 presents the Mechanical properties of polymer concrete. Table 2 shows the mix proportion of the polymer concrete matrix.

Six specimens are made and tested for each series of mixtures to confirm the accuracy of the results.

As pullout and direct tensile tests are performed on the specimens, the laboratory specimens were made in Dog Bone form and pullout specimens whose geometric specifications are shown in Fig. 1. Fig. 2 shows the specimens prepared for pullout and direct tensile testing.

2.1 Pullout test

The main reason for adding fibers to the composite matrix is to postpone and control crack formation and propagation. Studies show that the most significant effect of fibers is mostly after the cracks are formed. Fibers are placed as a bridge between cracks and prevent the sudden fracture of composite matrix. The effect of fiber is primarily related to interfacial behavior, which controls the performance of the material after cracking under pullout loads. This shows the significance of calculating and analyzing fiber pullout behavior. The pullout test was employed in this study to examine the fiber-matrix interphase strength. Fig. 3 shows the laboratory setup for the pullout test of polymer concrete specimens in the form of briquettes in which only single fiber is embedded. In the test, a displacement-control load was applied to the specimens with a rate of 1 mm/min. The test ended when the fiber was pulled out completely or when a fracture occurred. Fig. 4 shows the force-displacement diagram obtained from the experimental pullout test. It should also be noted that the force-displacement curve obtained from the experimental tests presented in Fig. 4 is the dominant behavior of one of the six pullout test specimens.

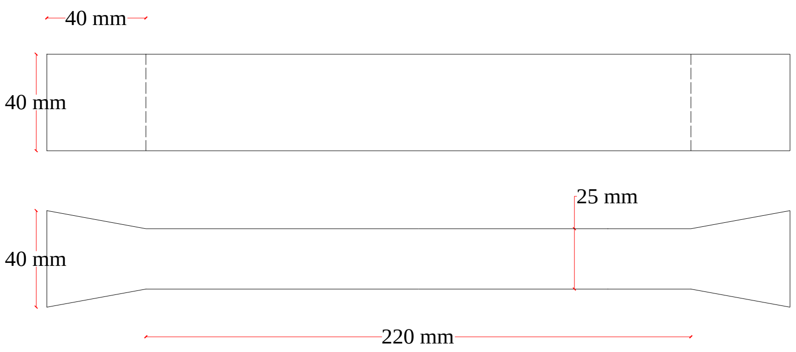

(a)

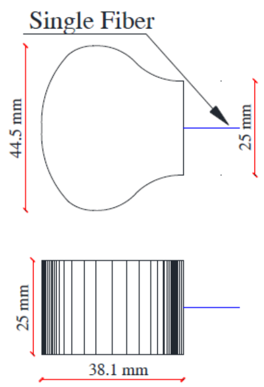

(b)

Fig. 1 The geometric specifications of (a) Dog Bone laboratory specimens (b) pullout specimens

(a)

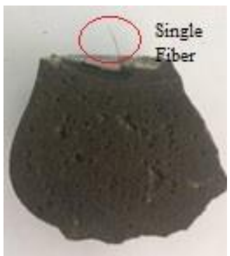

(b)

Fig. 2 The specimens for (a) direct tensile tests (b) single fiber pullout

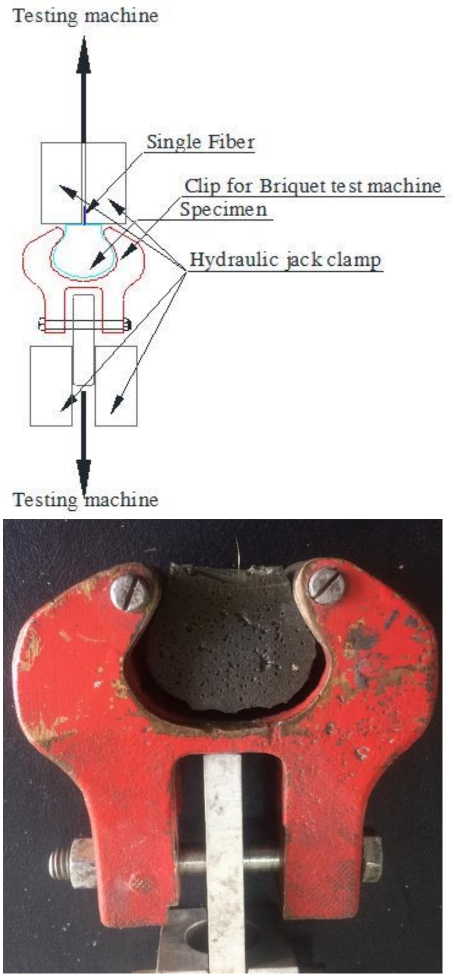

Fig. 3 Pullout testing setup

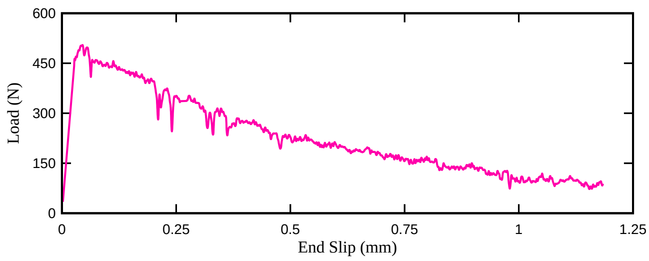

Fig. 4 Force-displacement diagram obtained from the experimental test results

2.2 Direct tensile test

A Universal unit with a capacity of 100 tons was used to perform direct tensile tests. The displacement control test was conducted at a rate of 0.5 mm/min. A Linear Variable Differential Transformer (LVDT) with a precision of 0.001 mm was used to record displacement. It measures the relative displacement between the two ends of a specimen, as shown in Fig. 5. The difference between the two relative displacements indicates the net displacement of the polymer composite specimen. To validate the finite-element results, steel-microfiber-reinforced polymer concrete specimens with 0, 1, and 2 vol% fibers content and an aspect ratio of 60 were tested under direct tensile.

Fig. 5 Setup to perform direct tensile tests

3. Meso-scale finite-element modeling

The research mainly aims to develop the finite-element method to calculate the mechanical properties of fiber-reinforced polymer concrete and examining the effect of geometric parameters of the fibers on its mechanical behavior. In the developed finite-element model, the steel-microfiber-reinforced polymer concrete comprises two components, namely the steel microfiber and the polymer concrete. The steel microfibers are assumed as the cylinders with certain diameter and length, which were considered to examine the effect of different aspect ratios. A polymer concrete was considered as a rectangular cube with homogeneous and uniform materials whose mechanical properties were determined after performing the experimental test on the laboratory specimens. To make the composite geometric model, the fibers were created in the model using random distribution. Then the created model volume was removed from the cube of the polymer concrete model.

3.1 Creating randomly-distributed fibers

Digimat commercial code was used to model the fibers with random distribution. Digimat MF is a Meso-scale modeling tool for materials and is based on Eshelby's single inclusion solution and Mori-Tanaka model for micromechanical analysis. The available code parameters can determine the size, distribution, and position of particles in a matrix. As regards, one of the aims of this study was to examine the effect of fibers content and aspect ratio, on the mechanical behavior of polymer concrete. The fibers with aspect ratios of 30, 60, and 90 were created considering a 0.2 mm diameter for the fibers. Aspect ratio and the volume fraction of fibers is defined in Digimat software, and by considering the values of these two parameters, the number of microfibers is determined to satisfy the defined conditions. Three microfibers contents were assumed, namely 0, 1, and 2 vol%. For example, Fig. 6 shows the creation of fibers with random distribution for the fibers with an aspect ratio of 60 and two volume fractions of 1 and 2. It shows that the fibers were distributed in the specimen

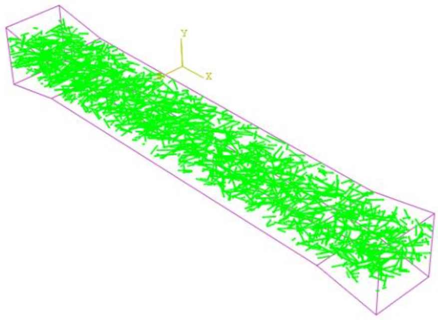

(a)

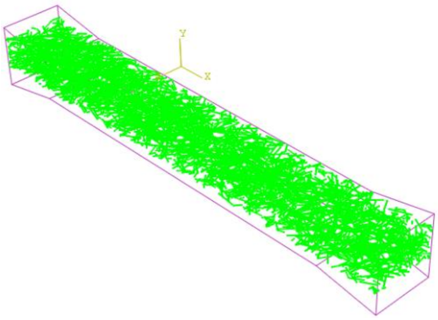

(b)

Fig. 6 Creating the randomly-distributed microfibers with aspect ratio of 60 (a)1 vol% and (b) 2 vol%

volume, and the dispersion is in a way that no fibers interfere with each other.

3.2 Defining fiber-composite interactions

The Cohesive Zone Model (CZM), which is based on force-displacement diagrams, was used for modeling the damage and separation phenomenon at the microfiber-composite interface. As stated, the force-displacement diagram parameters used in the finite-element model were obtained from the results of the pullout test conducted on a specimen of the polymer concrete. In the CZM, the crack behavior is expressed by the tension-separation law, which indicates the relationship between the stress and displacement of two cohesive surfaces. Material properties are defined in the CZM in exponential and bilinear forms, each offering unique potential functions. This study analyzes the rupture of the fiber-composite bond using cohesive surfaces in ABAQUS. The mechanical behavior of the contact surface is simulated by the tension-separation law based on its exponential model. As illustrated in Fig. 7, the contact surface behavior is assumed linear in the absence of failure, and the linear behavior disappears with the occurrence of each failure. It is assumed in the model that two parameters can consider all the mechanisms of microstructure and fracture process: (A) Maximum shear stress or cohesive zone strength (τ_{max}), (B) Separation at the maximum stress point (S_{max}). For the values exceeding maximum critical separation strain, the cohesive surface loses its stress tolerance capacity and cracks extension. In addition, G_c, which is interface fracture energy, is considered as another parameter for CZM. Since loading on fibers is in a combination mode in this problem, both

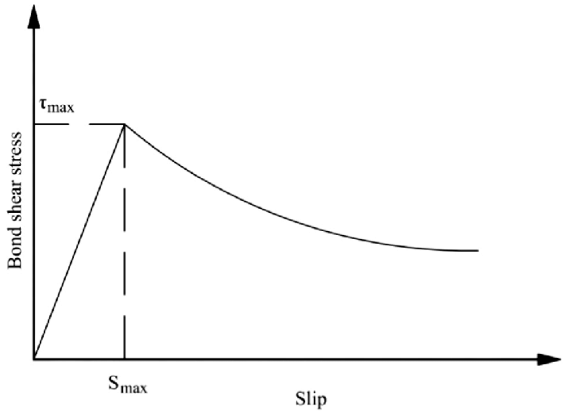

Fig. 7 Schematics shear stress in the cohesive zone versus slip

tangential and vertical stresses of contact participate in fracture energy, and the exponential relationship of fracture energy is as follows

$$\left(\frac{G_n}{G_{cn}}\right)^2 + \left(\frac{G_t}{G_{ct}}\right)^2 = 1 \tag{1}$$

Where G_n and G_t are the vertical and tangential fracture energies, respectively, they are equal to the area under the force-displacement diagram, and can be determined by the following equations

$$G_n = \int_0^{\delta_c} \sigma_n(\delta)\mathrm{d}\delta \tag{2}$$

$$G_t = \int_0^{\delta_c} \tau_t(\delta)\mathrm{d}\delta \tag{3}$$

3.3 Finite-element simulations

3.3.1 Finite-element pullout model

One of the important parameters in Meso-scale modeling is the appropriate interaction simulation among different components of the composite. Given the main aim of this study, which is discussing the effect of the incorporation of steel microfibers on the mechanical properties of the polymer concrete, the most notable point of the simulation is to determine fiber-polymer concrete cohesive specifications. Accordingly, the CZM parameters were determined through calibrating the finite-element model and the experimental results derived from the pullout test. Loading on the fiber is of the control displacement type, and displacement changes are imposed on the finite-element specimens with a rate of 0.2 mm/min. Eight-node C3D8R cubic elements were used for meshing polymer concrete and steel fiber. Fig. 8 shows the finite-element model for the pullout test of a steel microfiber.

3.3.2 Finite-element model for direct tensile test

The dog bone specimen shown in Fig. 6 is exposed to tensile loading at both ends in order to study the tensile behavior of polymer concrete. A dynamic/explicit solution method is used to observe the polymer concrete failure

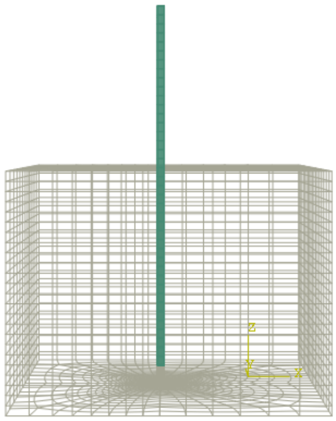

Fig. 8 The finite-element model for the steel microfiber pullout test

Table 3 The mechanical specifications of the steel microfiber

Diameter (mm)	Density (kg=m^3)	Modulus of Elasticity	Poisson's Ratio	Yield Stress (MPa)
0.2	7850	198	0.28	1480

Table 4 CZM parameters to define steel microfiber-polymer concrete interaction

τ_{max}	S_{max}	n
1.85 GPa	3×10^{-3}	0.2

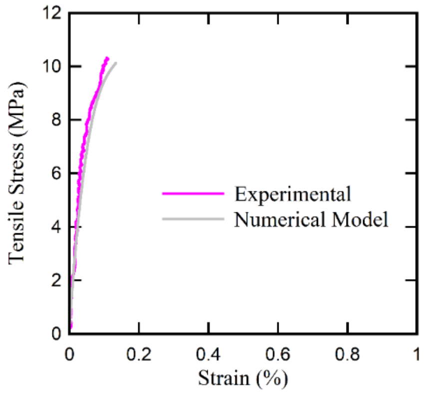

Fig. 9 Comparison between the experimental results and numerical model for direct tensile test of plain polymer concrete

mode. For this purpose, loading on the specimens was applied with a rate of 0.5 mm/min. The mechanical properties of the polymer concrete are defined using the results of the experimental tests in Section 2. Since the aggregates used in the polymer composite mixture provided in this study are fine silica sand (maximum diameter of 2.36 mm) and are distributed almost uniformly, therefore the material used is considered homogeneous. Also, since the element deletion method is used in this study, the presented coding removes the elements in which the maximum stress yields to the stress value. An elastic-plastic model was used for the steel fibers which their specifications are presented in Table 3.

The fiber-composite interactions were modeled using the contact bond and by defining cohesive elements. The theory of maximum stress is used in the present study to identify the interaction between the fibers and the matrix.

The maximum principal stress criterion can be represented as

$$f = \left\{ \frac{\langle \sigma_{max} \rangle}{\sigma^o_{max}} \right\} \tag{4}$$

Here, σ^o_{max} represents the maximum allowable principal stress. The symbol <> represents the Macaulay bracket with the usual interpretation. The Macaulay brackets are used to signify that a purely compressive stress state does not initiate damage. Damage is assumed to initiate when the maximum principal stress ratio (as defined in the expression above) reaches a value of one. Since all the stress tensor components are involved in the calculation of the maximum stress value, this criterion will also be applied to the fracture of the mixed-mode.

The CZM parameters were specified in a way that the force-displacement obtained from the finite-element model conforms to the experimental results of the steel fiber pullout test. After calibrating the model with pullout test results, the CZM was characterized by the results presented in Table 4.

4. The materials mechanical properties and the validation of the numerical model

4.1 The mechanical properties used in the finite-element model

As stated, the mechanical properties of the polymer concrete used in this study were determined by the direct tensile test, and they were then used as an input for the finite-element model. The mechanical properties have been derived from the stress-strain curve obtained from the experimental test on the plain polymer concrete specimen. Fig. 9 shows the stress-strain curve achieved by the experimental test results and the finite-element model on the plain polymer concrete. The results were derived after calibration of the finite-element model with the experimental test results. The results show that the finite-element model estimates the polymer concrete behavior under tensile loading with appropriate accuracy. Also, it models mechanical behavior around the fracture area almost without any error. However, by approaching the yield stress, the difference between the finite-element model and the experimental results reaches approximately 5.4%. Based on the experimental results and the results of the finite-element model, the tensile strengths of the polymer concrete are 10.57 MPa and 9.99 MPa, respectively.

In the following step and in order to model the microfiber-polymer adhesion in the composite, the interface area properties were determined by calibrating the numerical values of CZM model parameters with the experimental results for the pullout test applied on single microfiber. Fig. 10 demonstrates the force-displacement

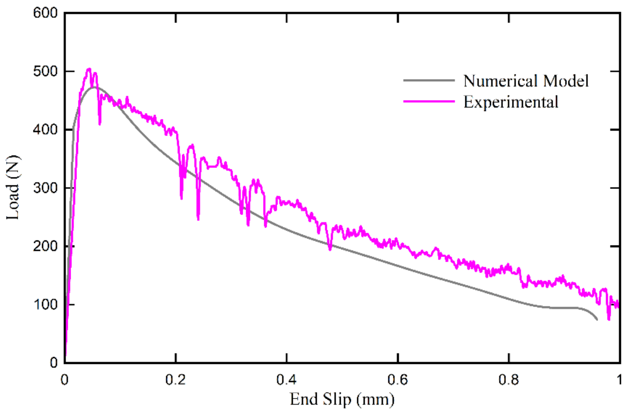

Fig. 10 Force-displacement diagrams of the microfiber pullout test, plotted using experimental results and the finite-element model

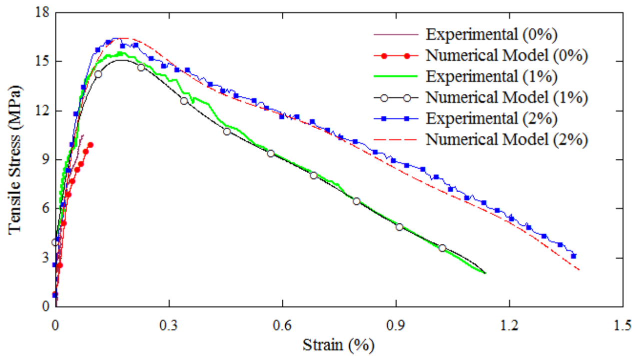

Fig. 11 The stress-strain diagram for the specimens obtained from direct tensile experimental test and finite-element simulation

diagram plotted using the experimental results of the microfiber pullout test and also the finite-element model. As it shows, after calibrating the CZM model parameters, the finite-element results are in agreement with the experimental ones with an approximately 4% error for the highest slip force. After calibrating the finite-element model and determining the CZM parameters, the constants of the fiber-polymer adhesion model were achieved (Table 4).

The load-end slip curve derived from the fibers' pullout test can be divided into three stages. As it can be observed in Figure 10, the first stage of the curve is linear up to the first crack occurred in the interfacial transition zone (ITZ) of the fiber and matrix. After the appearance of the initial crack, it begins to propagate in ITZ of the fiber and matrix. In this step, the slip force at the fiber and matrix intersection and the cohesive force in the crack-free zone resist the external load. Increasing the external load leads to a relative increase in the slip force in the detached zone. By increasing the external load value up to the ultimate point, the restrained zone of fiber becomes very short, and the complete pullout failure occurs. The only resisting internal force in this step is the fiber-matrix slip force. It becomes clear that this section is gradually eliminated as long as the fiber pullouts from the matrix. Fig. 10 shows that the maximum microfiber pullout force is 504 N that corresponds to a displacement of 0.04 mm.

4.2 Validating the model

After determining the polymer concrete specifications and the properties of the microfiber-composite cohesive zone, this section addresses the validation of the Meso-scale finite-element model. For this purpose, the experimental tests were carried out on microfiber-reinforced polymer concrete specimens with 0, 1, and 2 vol% fiber contents. Fig. 11 shows the stress-strain diagram for the specimens obtained from the results of the direct tensile experimental tests and the Meso-scale finite-element simulation. The results suggest compatibility between the Meso-scale finite-element model and the experimental results. Fig. 11 shows that the estimation errors of tensile strength for the specimens using the Meso-scale finite-element method are respectively 4%, 2.5%, and 1%.

Another capability of the Meso-scale finite-element model is to estimate the fracture zone in structural elements, which can be put into use without any experimental testing. Fig. 12 compares the fracture zone of the specimen with 1% of microfiber. As it shows, the zone and the fracture mode

(a)

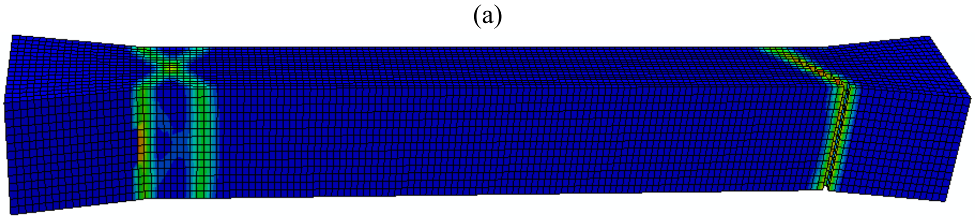

(b)

Fig. 12 Comparison of the fracture zone of the specimen with 1% microfiber (A) the results for the direction tensile experimental test and (B) Meso-scale finite-element model

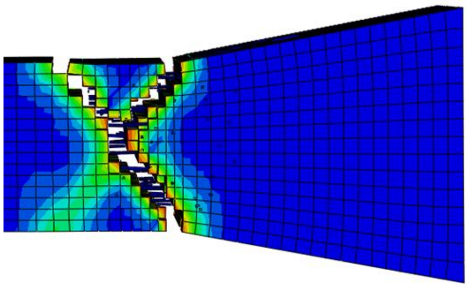

Fig. 13 The fracture zone of the polymer concrete with 2% of steel microfiber

in the numerical modeling have acceptable compatibility with the experimental results. Numerical and experimental results of the direct tensile tests showed that the fracture occurred in the transition zone of the dog-bone specimens. These results could be due to the strengths values obtained are associated with the stress concentration produced by the presence of a corner. This type of fracture patterns in the transient zone was observed for all experimental and numerical specimens, indicating the accuracy of the modeling. On the other hand, since the main purpose of this research is to present a more precise finite element model using the random distribution of fibers. Therefore, due to the excellent agreement between experimental and finite element results, the type of fracture does not cause any problem to the results accuracy.

Based on this, the numerical model can be used to estimate the mechanical properties and the behavior of polymer concrete conveniently and precisely for a wide range of different effective parameters. Fig. 13 shows a zoomed view of the fracture zone of the finite-element model for the specimen with 2% of microfiber. It can be seen that the presence of microfiber causes further bonding of the composite, which increases composite strength after the first crack occurrence.

4.3 Effect of steel microfiber properties

This section discusses the effects of the steel microfiber content and aspect ratio on polymer concrete properties using the 3D Meso-scale finite elements model. The polymer concrete analyzed at three microfiber contents of (0, 0.5, 1, and 2 vol%), and three different aspect ratios of (30, 60, and 90). In all the simulations, fiber diameter was considered fixed (0.2 mm) and the fiber length was considered variable in proportion to the aspect ratio.

The tensile stress-strain diagrams plotted using the results derived from the Meso-scale finite-element model are presented in Figs. 14-16 for different microfiber contents (vol%) and aspect ratios. The results indicate that the tensile strength of the steel-microfiber-reinforced polymer concrete is considerably higher than that of the plain specimens. The incorporation of fiber affects the polymer concrete behavior significantly; and then, prevents a brittle fracture of the composite. Accordingly, the stress-strain diagrams of the fiber-reinforced specimens have a slight slope after ultimate tensile strength (UTS) and feature no sudden drop. Based on this, the presence of fibers

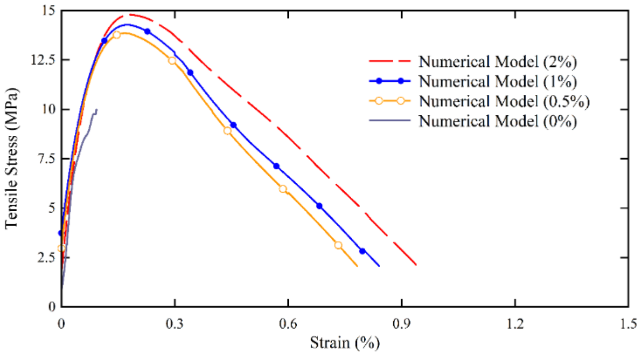

Fig. 14 The tensile stress diagram versus strain obtained from the meso scale finite-element results for steel-microfiber-reinforced polymer concrete with aspect ratio of 30

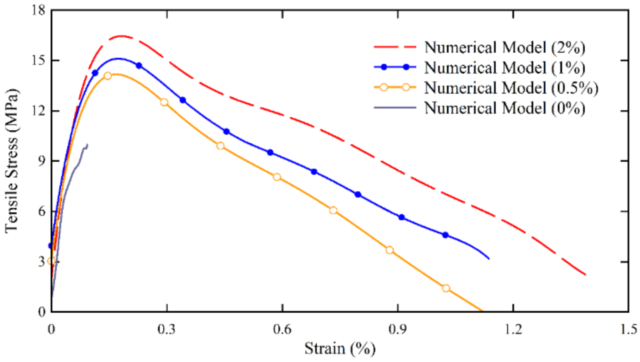

Fig. 15 The tensile stress diagram versus strain obtained from the meso scale finite-element results for steel-microfiber-reinforced polymer concrete with aspect ratio of 60

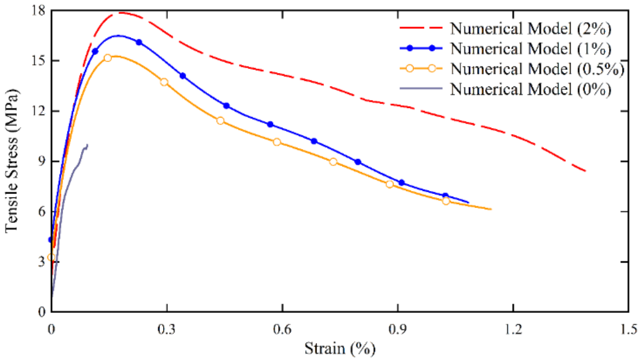

Fig. 16 The tensile stress diagram versus strain obtained from the meso scale finite-element results for steel-microfiber-reinforced polymer concrete with aspect ratio of 90

strengthens polymer concrete bonding after fracture; prevent the rapid development of cracks, and increases energy absorption capacity. Moreover, incorporating fibers into polymer concrete improves the tensile strength of the specimens. For example, considering the results presented for the microfiber-reinforced polymer concrete with the aspect ratio of 30, the tensile strengths of the polymer concrete with 0%, 0.5%, 1%, and 2% of microfiber are 9.99 MPa, 13.85 MPa, 14.27 MPa, and 14.78 MPa, respectively.

Table 5 The UTS and deformation corresponding to different microfiber contents

Aspect ratio		Fiber content (by volume)			
		Plain	0.5%	1%	2%
30	Peak stress (MPa)	9.99	13.85	14.27	14.78
	Peak deformation (mm)	0.092	0.158	0.174	0.177
60	Peak stress (MPa)	9.99	14.16	15.1	16.44
	Peak deformation (mm)	0.092	0.165	0.181	0.184
90	Peak stress (MPa)	9.99	15.27	16.48	17.86
	Peak deformation (mm)	0.092	0.172	0.185	0.195

It is observed that the composite's tensile strength increases relatively with the increase in the aspect ratio of the fibers. However, the most remarkable point is the different behavior of the specimens in the softening zone of the diagrams for different aspect ratios. At higher aspect ratios, the slope of the stress-strain diagram decreases after UTS, which increases the energy absorption of the polymer concrete.

Table 5 shows the corresponding UTS and deformation of the specimens. The results show that ultimate tensile strength and strain are greater for longer fiber, which means that the strength of the fiber reinforced specimens exceeds the plain ones. At a fixed fiber diameter, fiber length raise with increasing the aspect ratio. Therefore, the adhesive fiber-polymer contact area is increased at higher aspect ratios, thus requiring more energy to completely separate fibers from the composite. For example, at 1 vol% microfiber content, the tensile strength of polymer concrete specimens raises by nearly 18% with increasing the aspect ratio from 30 to 90. Based on this, the increase of aspect ratio improves the performance of polymer concrete after the initial cracks appeared.

5. Conclusions

A 3D Meso-scale finite-element model with randomly-distributed fibers was presented to study the mechanical behavior of polymer concrete reinforced with steel microfiber. The experimental tests achieved the main mechanical properties of polymer concrete essential for finite element modeling. The numerical model parameters expressing the cohesive behavior between microfiber and polymer concrete were determined using the microfiber pullout test. The effect of fiber characteristics on the mechanical properties of polymer concrete was discussed after verifying the accuracy of the results of the developed Meso-scale finite-element model in comparison with the experimental results. The results indicate that the Meso-scale finite-element model developed in this research estimates the mechanical specifications of polymer concrete and provides the fracture mode of the specimens with appropriate accuracy. Also, the characteristics of the fibers have a significant impact on the mechanical behavior of the steel-microfiber-reinforced polymer concrete as the UTS increases by nearly 18% with increasing the aspect ratio from 30 to 90. The proposed Meso-scale finite-element model can be conveniently applied to different types of composites incorporating different fibers under various geometric and loading conditions.

Since all the stress tensor components are involved in the calculation of the maximum stress value, this criterion will also be applied to the fracture of the mixed-mode. Therefore, the results of the simulation are not solely related to fracture of second-mode, and indeed represent the effects of mixed-mode.

References

Abdel-Fattah, H. and El-Hawary, M.M. (1999), "Flexural behavior of polymer concrete", *Constr. Build. Mater.*, **13**(5), 253-262. https://doi.org/10.1016/S0950-0618(99)00030-6.

Aslani, F. and Nejadi, S. (2012), "Bond characteristics of steel fibre reinforced self-compacting concrete", *Can. J. Civil Eng.*, **39**(7), 834-848. https://doi.org/10.1139/l2012-069.

Ayatollahi, M., Shadlou, S. and Shokrieh, M. (2011), "Multiscale modeling for mechanical properties of carbon nanotube reinforced nanocomposites subjected to different types of loading", *Compos. Struct.*, **93**(9), 2250-2259. https://doi.org/10.1016/j.compstruct.2011.03.013.

Bouhala, L., Makradi, A., Belouettar, S., Younes, A. and Natarajan, S. (2015), "An XFEM/CZM based inverse method for identification of composite failure parameters", *Comput. Struct.*, **153**, 91-97. https://doi.org/10.1016/j.compstruc.2015.02.035.

Budhe, S., Banea, M., De Barros, S. and Da Silva, L. (2017), "An updated review of adhesively bonded joints in composite materials", *Int. J. Adhes. Adhes.*, **72**, 30-42. https://doi.org/10.1016/j.ijadhadh.2016.10.010.

Du, C., Jiang, S., Qin, W., Xu, H. and Lei, D. (2012), "Reconstruction of internal structures and numerical simulation for concrete composites at mesoscale", *Comput. Concrete*, **10**(2), 135-147. https://doi.org/10.12989/cac.2012.10.2.135.

Gencel, O., Brostow, W., Martinez-Barrera, G. and Gok, M.S. (2012), "Mechanical properties of polymer concretes containing different amount of hematite or colemanite", *Polim.*, **57**(4).

Hassani Niaki, M., Fereidoon, A. and Ghorbanzadeh Ahangari, M. (2018), "Mechanical properties of epoxy/basalt polymer concrete: Experimental and analytical study", *Struct. Concrete*, **19**(2), 366-373. https://doi.org/10.1002/suco.201700003.

Isla, F., Ruano, G. and Luccioni, B. (2015), "Analysis of steel fibers pullout. Experimental study", *Constr. Build. Mater.*, **100**, 183-193. https://doi.org/10.1016/j.conbuildmat.2015.09.034.

Jafari, K., Tabatabaeian, M., Joshaghani, A. and Ozbakkaloglu, T. (2018), "Optimizing the mixture design of polymer concrete: An experimental investigation", *Constr. Build. Mater.*, **167**, 185-196. https://doi.org/10.1016/j.conbuildmat.2018.01.191.

Karimzadeh, F., Ziaei-Rad, S. and Adibi, S. (2007), "Modeling considerations and material properties evaluation in analysis of carbon nano-tubes composite", *Metal. Mater. Tran. B*, **38**(4), 695-705. https://doi.org/10.1007/s11663-007-9065-y.

Khani, N., Yildiz, M. and Koc, B. (2016), "Elastic properties of coiled carbon nanotube reinforced nanocomposite: a finite element study", *Mater. Des.*, **109**, 123-132. https://doi.org/10.1016/j.matdes.2016.06.126.

Martínez-Barrera, G., Menchaca-Campos, C. and Gencel, O. (2013), "Polyester polymer concrete: Effect of the marble particle sizes and high gamma radiation doses", *Constr. Build. Mater.*, **41**, 204-208. https://doi.org/10.1016/j.conbuildmat.2012.12.009.

Martinez-Barrera, G., Vigueras-Santiago, E., Gencel, O. and Hagg Lobland, H.E. (2011), "Polymer concretes: a description and

methods for modification and improvement", *J. Mater. Educat.*, **33**(1), 37.
Moodi, F., Kashi, A., Ramezanianpour, A.A. and Pourebrahimi, M. (2018), "Investigation on mechanical and durability properties of polymer and latex-modified concretes", *Constr. Build. Mater.*, **191**, 145-154. https://doi.org/10.1016/j.conbuildmat.2018.09.198.
París, F., Correa, E. and Mantič, V. (2017), "Micromechanical evidences on interfibre failure of composites", *Structural Integrity of Carbon Fiber Composites*, Springer, 359-390.
Rebeiz, K., Serhal, S.and Craft, A. (2004), "Properties of polymer concrete using fly ash", *J. Mater. Civil Eng.*, **16**(1), 15-19. https://doi.org/10.1061/(ASCE)0899-1561(2004)16:1(15).
Reis, J. (2006), "Fracture and flexural characterization of natural fiber-reinforced polymer concrete", *Constr. Build. Mater.*, **20**(9), 673-678. https://doi.org/10.1016/j.conbuildmat.2005.02.008.
Reis, J. and Ferreira, A. (2004), "Assessment of fracture properties of epoxy polymer concrete reinforced with short carbon and glass fibers", *Constr. Build. Mater.*, **18**(7), 523-528. https://doi.org/10.1016/j.conbuildmat.2004.04.010.
Sett, K. and Vipulanandan, C. (2004), "Properties of polyester polymer concrete with glass and carbon fibers", *Mater. J.*, **101**(1), 30-41.
Shannag, M.J., Brincker, R. and Hansen, W. (1997), "Pullout behavior of steel fibers from cement-based composites", *Cement Concrete Res.*, **27**(6), 925-936. https://doi.org/10.1016/S0008-8846(97)00061-6.
Shokrieh, M., Rezvani, S. and Mosalmani, R. (2017), "Mechanical behavior of polyester polymer concrete under low strain rate loading conditions", *Polym. Test.*, **63**, 596-604. https://doi.org/10.1016/j.polymertesting.2017.09.015.
Smolčić, Ž. and Ožbolt, J. (2017), "Meso scale model for fiber-reinforced-concrete: Microplane based approach", *Comput. Concrete*, **17**(4), 375-385. https://doi.org/10.12989/cac.2017.19.4.375.
Soetens, T., Van Gysel, A., Matthys, S. and Taerwe, L. (2013), "A semi-analytical model to predict the pullout behaviour of inclined hooked-end steel fibres", *Constr. Build. Mater.*, **43**, 253-265. https://doi.org/10.1016/j.conbuildmat.2013.01.034.
Tam, L.H. and Lau, D. (2016), "Effect of structural voids on mesoscale mechanics of epoxy-based materials", *Multisc. Multiphys. Mech*., **1**(2), 127-141. https://doi.org/10.12989/csm.2016.5.4.355.
Tregger, N., Corr, D., Graham-Brady, L. and Shah, S. (2007), "Modeling mesoscale uncertainty for concrete in tension", *Comput. Concrete,* **4**(5), 347-362. https://doi.org/10.12989/cac.2007.4.5.347.
Tuyan, M. (2012), "Pullout behavior of single steel fiber from SIFCON matrix", *Constr. Build. Mater.*, **35**, 571-577. ttps://doi.org/10.1016/j.conbuildmat.2012.04.110.
Velasco, M., Graciani, E., Távara, L., Correa, E. and París, F. (2018), "BEM multiscale modelling involving micromechanical damage in fibrous composites", *Eng. Anal. Bound. Elem.*, **93**, 1-9. https://doi.org/10.1016/j.enganabound.2018.03.012.
Vogt, F., Gypser, A., Kleiner, F. and Osburg, A. (2018), "Polymer concrete for a modular construction system: Investigation of mechanical properties and bond behaviour by means of X-ray CT", *International Congress on Polymers in Concrete,* Springer.
Wang, L. and Bao, J. (2015), "Mesoscale computational simulation of the mechanical response of reinforced concrete members", *Comput. Concrete*, **15**(2), 305-319. https://doi.org/10.12989/cac.2015.15.2.305.